Journal of Taibah University Medical Sciences (2023) 18(6), 1244–1253

Taibah University

Journal of Taibah University Medical Sciences

www.sciencedirect.com

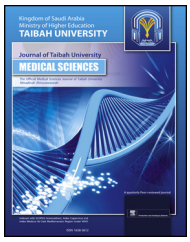

Original Article

New drug-like small molecule antagonizes phosphatidylinositol (3,4,5)-trisphosphate (PIP3) in patients with conotruncal heart defects

Alaaeldin G. Fayez, PhD [a,*], Nora N. Esmaiel, PhD [a], Engy A. Ashaat, MD [b], Miral M. Refeat, PhD [c], Randa S. Lotfy, PhD [a], Haiam Abdel Raouf, PhD [d] and Mona O. El Ruby, MD [b]

[a] *Molecular Genetics and Enzymology Department, Human Genetics and Genome Research Institute, National Research Centre, Giza, Egypt*
[b] *Clinical Genetics Department, Human Genetics and Genome Research Institute, National Research Centre, Giza, Egypt*
[c] *Medical Molecular Genetics Department, Human Genetics and Genome Research Institute, National Research Centre, Giza, Egypt*
[d] *Immunogenetics Department, Human Genetics and Genome Research Institute, National Research Centre, Giza, Egypt*

Received 18 September 2022; revised 2 February 2023; accepted 20 April 2023; Available online 4 May 2023

الملخص

أهداف البحث: عيوب القلب الوعائية وراثية بشكل كبير وحوالي ثلث عيوب القلب الخلقية ناتجة عن عيوب القلب الوعائية. باستخدام التحليل اللاحق لعيوب القلب المخروطية -بيانات دراسة الترابط الجينومي الكامل ذات الصلة، تم افتراض مسار جديد مفترض لنقل الإشارات، يسمى "فارس2-بك3كا-أ ك ت"، المرتبط بعيوب القلب الوعائية. كنا نهدف بشكل أساسي إلى التحقق من مسار "فارس2-بك3كا-أ ك ت" بشكل تجريبي باستخدام المقياسين "فارس2" و "بيب3" في كل من مرضى عيوب القلب والعينة الضابطة، وإنشاء مثبط "بيب3"، كواحد من مسببات عيوب القلب الضارة ذات الصلة، باستخدام استراتيجية تصميم الأدوية القائمة على "أ ك ت".

طرق البحث: تم إجراء التنميط الجيني "ار اس 2517582" والتعبير النسبي لـ "فارس2" في 207 أفراد باستخدام تفاعل البلمرة المتسلسل الكمي، إلى جانب ذلك تم أيضا قياس "بيب3" المحررة في البلازما لدى 190 فردا باستخدام تقنية المقايسة الامتصاصية المناعية للإنزيم المرتبط. استخدمنا نموذج ميزات "أ ك ت"-حامل الخاصة الدوائية لاكتشاف خصم "بيب3" باستخدام أدوات حسابية متعددة وأدوات تقدير شبيهة بالعقاقير.

النتائج: تم تأكيد إمراض عيوب القلب الوعائية بسبب فرط التحفيز المفرط لـ "فارس2-بك3كا-أ ك ت" عن طريق "فارس2" المرتفع و "بيب3" في مرضى عيوب القلب الوعائية. حددنا جزيئا صغيرا جديدا، يسمى "بيسب322"، قادرا على أن يقاوم ارتباط "بيب3"، وتم منحه الأولوية من خلال الفحص الافتراضي لـ 21 جزيئا صغيرا افتراضيا. أظهر "بيسب322" الحد الأدنى من التغير النسبي لاختلاف موقع جزيئاته "رمسد"، وتقارب ربط عال، وثابت تفكك أقل من مجمع بيب3-أ ك ت" بمقدار 1.99 كيلو كالوري/مول مما يؤدي إلى تحول التوازن التفضيلي نحو تكوين معقد "بيسب322-أ ك ت". عرضت "بيسب322" الخصائص الدوائية المقبولة وخصائص تشابه الأدوية وفقا لقاعدة ليبينسكي و قاعدة امتصاص وتوزيع وتمثيل الغذاء وإفرازه المكونة من خمسة مصنفات. هذا هو أول جزيء محتمل كشبيه علاجي الدواء لمرضى عيوب القلب الوعائية الذين يعانون من ارتفاع "بيب3".

الاستنتاجات: "بيب3" هي مؤشرات حيوية تشخيصية مفيدة لمرضى عيوب القلب. يعد نموذج ميزات "أ ك ت"-حامل الخاصة الدوائية نهجا ممكنا لاكتشاف المزيد من مضادات تأثير"بيب3". يوصى بإجراء المزيد من اختبارات التطوير لجزئ "بيسب322".

الكلمات المفتاحية: بروتين أ ك ت؛ عيوب القلب الوعائية؛ تصميم الأدوية؛ مضاد "بيب3"؛ مقطع مشابه بليكسترن؛ مسارنقل الإشارة

Abstract

Objectives: Conotruncal heart defects (CTDs) are highly heritable, and approximately one-third of all congenital heart defects are due to CTDs. Through post-analysis of GWAS data relevant to CTDs, a new putative signal transduction pathway, called Vars2-Pic3ca-Akt, associated with CTD has been hypothesized. Here, we aimed to validate the Vars2-Pic3ca-Akt pathway experimentally by measuring Vars2 and PIP3 in patients with CTDs and controls, and to construct a PIP3 inhibitor, as one of harmful-relevant CTD pathogenesis, through an Akt-based drug design strategy.

Methods: rs2517582 genotype and relative Vars2 expression in 207 individuals were determined by DNA sequencing and qPCR respectively, and free plasma PIP3

* Corresponding address: Molecular Genetics and Enzymology Department, 33 El Buhouth st. Giza, Dokki, P.O.12622, Egypt.
E-mail: afayez_nrc@yahoo.com (A.G. Fayez)

Peer review under responsibility of Taibah University.

ELSEVIER Production and hosting by Elsevier

 https://doi.org/10.1016/j.jtumed.2023.04.006

in 190 individuals was quantified through ELISA. An Akt-pharmacophore feature model was used to discover PIP3 antagonists with multiple computational and drug-like estimation tools.

Results: CTD pathogenesis due to Vars2-Pic3ca-Akt overstimulation was confirmed by elevated Vars2 and PIP3 in patients with CTDs. We identified a new small molecule, 322PESB, that antagonizes PIP3 binding. This molecule was prioritized via virtual screening of 21 hypothetical small molecules and it showed minimal RMSD change, high binding affinity andlower dissociation constant than PIP3-Akt complex by 1.99 Kcal/Mol, thus resulting in an equilibrium shift toward 322PESB-Akt complex formation. Moreover, 322PESB exhibited acceptable pharmacokinetics and drug likeness features according to ADME and Lipinski's rule of five classifiers. This compound is the first potential drug-like molecule reported for patients with CTDs with elevated PIP3.

Conclusion: PIP3 is a useful diagnostic biomarker for patients with CTDs. The Akt-pharmacophore feature model is a feasible approach for discovery of PIP3 signalling antagonists. Further 322PESB development and testing are recommended.

Keywords: Akt; Conotruncal heart defects; Drug design; PIP3 antagonist; Pleckstrin homology domain; Signal transduction pathway

Introduction

Evolutionarily conserved genetic variants have been proposed as markers for quantitative trait locus analysis, and assessment of medically important differences in disease susceptibility and drug response.[1,2]

Genome-wide association study (GWAS) is a powerful and promising method for investigating the effects of genetic variations. Post-GWAS analysis is an index approach for understanding the mechanisms of action of variants, and consequently drug targets and effects. Sanseau et al. (2012) have reported that 21% of genes in the GWAS catalogue are amenable to drug modelling,[3] such as monoclonal antibodies against interleukin-12 designed for treatment of inflammatory bowel disease.[4]

Fayez (2018) has performed post-GWAS analysis and postulated the existence of a new hypothetical signal transduction pathway, consisting of Vars2, Pic3ca and Akt proteins, associated with CTD pathogenesis; however, further confirmation of this hypothesis is required.[5] Therefore, two biomarkers derived from the Vars2-Pic3ca-AKT pathway were assessed in the current study. Moreover, a bioactive small drug-like molecule was constructed.

Wang et al. (2008) have found a positive relationship between Vars2 and PI3k proteins in multicellular organisms.[6] Mendoza et al. (2011) have indicated that PIP3 generates as a result of PI3K recruitment for the kinase Akt protein into the plasma membrane.[7] Várnai et al. (2005) have reported that PIP3 target proteins are recruited to the plasma membrane through pleckstrin-homology (PH) domain-mediated binding to newly formed PIP3.[8]

Multiple PIP3-PH domain protein interactions have indicated that PIP3 is a key signalling messenger in multiple signal transduction-based biological processes. Both triciribine phosphate and nonphosphoinositide are small molecules described as potential tumor growth inhibitor drugs preventing binding of PIP3 to PH domain proteins.[9,10]

Drug design through computational methods is cost effective and producible hit generation. These computational methods can be classified into ligand-based and receptor-based methods. Pharmacophore identification models involve description of the necessary molecular features for recognition of a ligand by a corresponding receptor. The receptor-pharmacophore feature model uses complex crystal structures and extracts the necessary feasible interactions and selectivity constraints.[11]

Herein, we used a receptor (Akt)-pharmacophore feature model to identify the lead compounds which inhibit PIP3-PH domain Akt complex formation and thereby acting as PIP3 antagonists. In the current study, one drug-like small molecule passed the computational evaluation stage and absorption, distribution, metabolism, excretion and toxicity (ADME) evaluation, and it may be serve as a potential inhibitor of PIP3 binding to Akt. To our knowledge, no treatment for CTD has been approved to date.

Material and Methods

All participants' guardians provided written informed consent.

Study design

Our case-control study included 207 participants (105 patients with CTDs and 102 controls). Four patients were excluded because clinicians found that they had other associated non-cardiac anomalies. Relative Vars2 expression level was normalized to GAPDH expression in duplicate qRT-PCR runs, and plasma PIP3 was measured with ELISA. Subsequently, we used an Akt-pharmacophore feature model to design effective lead small molecule inhibitors for PIP3 binding to the PH domain of Akt. After sorting, the final inhibitor was evaluated with ADME and Lipinski's rule of five classifiers.

Clinical investigations

Full clinical examination was performed for each participant in the case and control groups, with an emphasis on the heart and cardiovascular system. Family history of any similarly affected person in each family and consanguinity were reported. Only patients with isolated CTD were included, and patients with known syndromic features combined with a CTD phenotype were excluded. The controls were individuals without cardiac anomalies and syndromic features.

Genotyping

PCR sequencing primers for amplifying the rs2517582 locus were designed with the NCBI Primer-BLAST tool (http://www.ncbi.nlm.nih.gov/tools/primer-blast).[12] Genotyping patterns of this locus were detected with Sanger sequencing with a QV $\geq$ 30 for a reference nucleotide at the heterogeneity state.

Relative quantitative real-time assay of Vars2 expression

Whole RNA from peripheral blood samples was extracted with QIAamp RNA Blood Mini kits (QIAGEN, Hilden, Germany) according to the manufacturer's instructions. RNA concentration and purity were measured with a spectrophotometer (NanoDrop, Thermo Fisher, Waltham, USA). Extracted RNA was reverse transcribed, and its concentration was measured. The relative expression of Vars2 with respect to GAPDH was calculated with the $2^{-\Delta\Delta Ct}$ method and transformed with the $\log_2$FC formula. Primer design for Vars2 was performed with the NCBI Primer-BLAST tool (http://www.ncbi.nlm.nih.gov/tools/primer-blast).[12]

Phosphatidylinositol 3,4,5 tri-phosphate assays

Phosphatidylinositol 3,4,5 tri-phosphate (PIP3), a major metabolite product of the Vars2-Pic3ca-Akt pathway, was assayed. Plasma PIP3 levels were measured with a PIP3 ELISA Kit (cat. No. ABIN4947941, antibodies-online GmbH, Germany) based on the competitive inhibition enzyme immunoassay technique.

Receptor-based pharmacophore feature model: structure-based approach

A receptor-based pharmacophore feature model was used to compute five pharmacophore features relevant to interactions between the PH domain of Akt and PIP3: (i) hydrogen bond acceptor, (ii) hydrogen bond donor, (iii) hydrophobicity, (iv) ionizability and (v) charge and solvent accessibility area. The PDB is a repository of 3-D structural data. Here, the high-resolution X-ray crystal structure for the PH domain of Akt-PIP3 was used (PDB ID 1H10; 1.4 Å). The five pharmacophore features were considered in the inhibitory small molecules identification. The pharmacophore features were computed and visualized with discovery studio visualizer.

Drug-like small molecule sorting and pharmacophore-based virtual screening

In-house, a database of 21 small molecules was generated. SwissADME[13] properties and Lipinski's rule of five[14] (under pH = 7.2 equivalent to cystolic cardiomyocyte pH value) were applied to exclude non-drug-like small molecules. SMILES descriptions of the small molecules were input into the SwissADME server. Most of the output ADME features were generated in one-panel bioavailability radar including lipophilicity, size, polarity, solubility, flexibility and saturation. Exclusion of non-drug-like molecules was performed before pharmacophore-based virtual screening. The virtual screening was performed with AutoDock Vina implemented in the SeamDock server.[15] Docking setting parameters included 1.0 Å spacing, five mode numbers and local docking coordinates (Centre: x: 1 Å; y: 10 Å; z: 7 Å. Size: x: 39 Å; y: 15 Å; z: 26 Å). We performed further sorting for docked molecules with docked binding affinity (dG), dissociation constant (Kd) and inhibition constant (Ki) values. The binding affinity was scored by kcal/mol. The differential binding affinity scores of docked PIP3 and the final sorted hit compound were computed with the neural network-based predictor KDEEP (in the PlayMolecule workspace).[16] Differential predicted scores of mean Kd, ligand efficiency, binding probability and mean Ki were also computed with KDEEP. The final sorted drug-like small molecule was named according to the IUPAC system with BIOVIA draw 2018,[17] and its topological features were computed with the SwissParam server.[18]

Binding characterization of BH domain/Akt with a final sorted drug-like small molecule

The physiochemical properties and bonding ability of the final sorted hit molecule were explored with the discovery studio visualizer tool.[17] The same tool was used to identify the active binding site and interacting pocket residues. The type and location of interacting residues and atoms were also detected. Radii and XYZ coordinates of the active binding site were calculated.

Similarity and off-target identification

The final sorted hit compound was subjected to similarity identification with SwissSimilarity (https://www.expasy.org/resources/swisssimilarity).[19] SwissSimilarity is part of the SwissDrugDesign workspace, and performs virtual ligand screening across very large-scale libraries of drugs, bioactive small molecules and commercially available compounds. To avoid any potential adverse effects, possible adverse effects and predicted off-target probabilities were computed with SwissTaegetPrediction.[20] A full flowchart of the stepwise method is shown in Figure 1.

Statistical analysis

The normality of Vars2 and PIP3 values was assessed with Kolmogorov–Smirnov, Shapiro–Wilk and robust M-estimator tests. The relative Vars2 expression was assessed on the basis of fold change (FC; $2^{-\Delta\Delta Ct}$) and transformed $\log_2$FC at significant $|\log_2 FC| \geq 1$ interval. The median was calculated as a tendency score. Means and standard deviations of the binding affinity and dissociation constant were computed. The Mann–Whitney test was used to evaluate median differences. Receiver operating characteristic curves were analyzed to compute a discriminator PIP3 cut-off point with index of union. $p < 0.05$ was considered significant. The statistical analysis was performed in PASW statistics (SPSS Inc. Released 2009. PASW Statistics for Windows, Version 18.0. Chicago).

Results

A total of 207 participants were investigated in the current study, comprising 105 patients with CTDs and 102 controls.

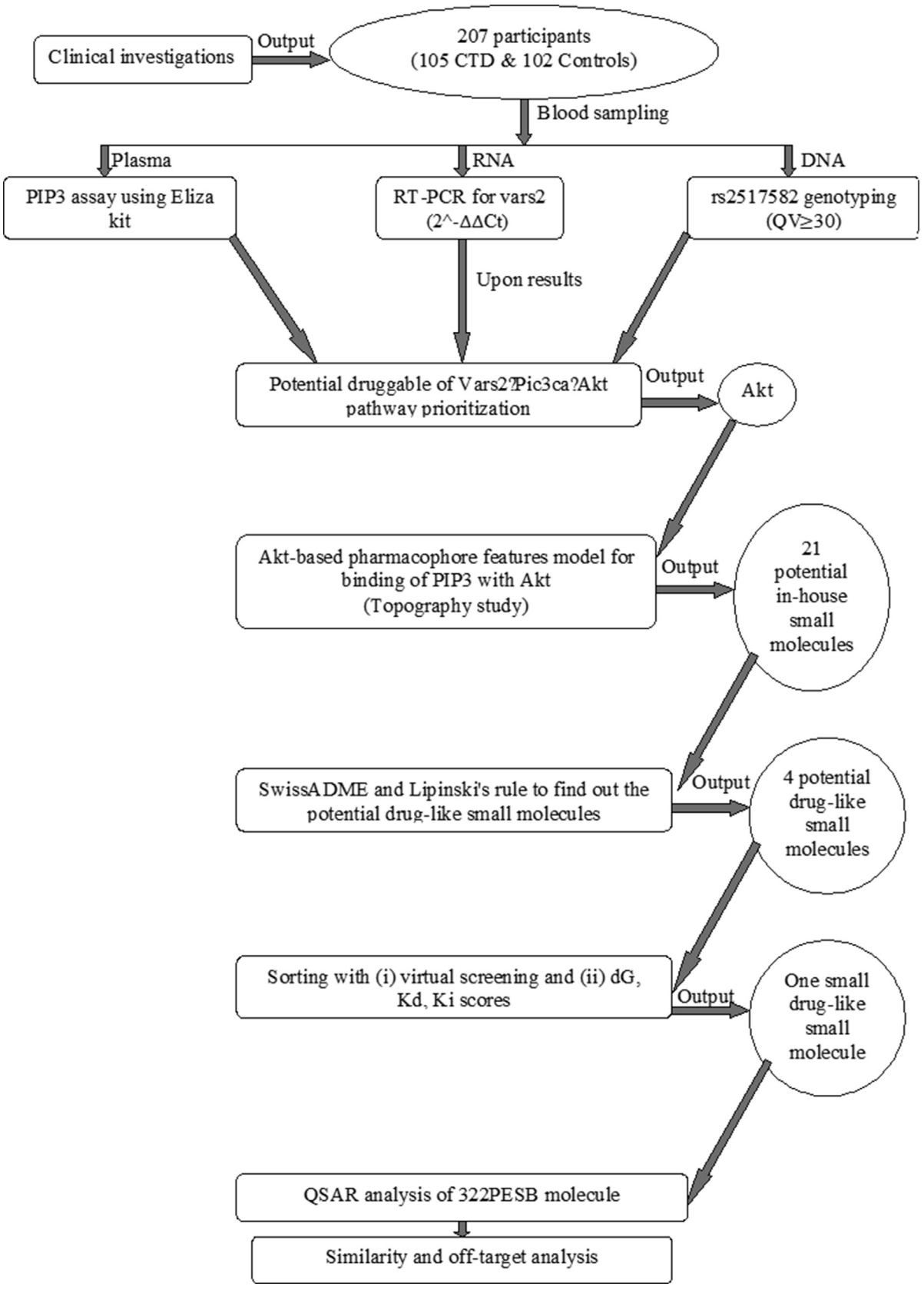

Figure 1: A full flowchart showing the stepwise procedures of the current study.

Table 1: Clinical characterization of patients with CTDs and controls.

Groups	N	Age (yrs)[a] Mean ± SD	Sex (%)	Consanguinity (%)
CTD	105	7 ± 2.5	Male: 49% Female: 51%	Positive (68%) Negative (32%)
Control	102	9 ± 3	Male: 55% Female: 45%	NA

[a] No statistically significant difference was found between the CTD and control groups in ages, p-value = 0.094.

Table 3: Difference in PIP3 amounts (ng/ml) among different rs2517582 genotypes.

Group		Patients		
		GG	GA	GA+AA
Controls	GG	Z = −1.374 P = 0.169[a]		
	GA		Z = −2.585 P = 0.010[a]	
	GA+AA			Z = −2.568 P = 0.010[a]

[a] This Asymp. Sig. (2-tailed) with Mann−Whitney test.

The clinical characteristics including the age and sex of the patients are shown in Table 1.

To determine proper statistical test sets according to the output Vars2 and PIP3 values, we tested normality with Kolmogorov−Smirnov and Shapiro−Wilk tests, which indicated that both Vars2 and PIP3 values did not follow a normal distribution. Robust alternatives of mean and median values locations were generated with the M-estimator test, which yielded scores closer to the median than the mean. Therefore, median-based tests were deemed most appropriate in the subsequent statistical analysis.

Vars2 expression is threefold higher in patients with CTDs than controls

We performed qPCR with duplicate reactions to determine the Vars2 mRNA expression in peripheral blood samples of patients with CTDs and controls. By applying an Fold change (FC) criterion to assess differential Vars2 expression between the CTD and control groups, normalized to GAPDH, the relative fold expression change of vars2 was threefold higher in patients with CTDs than controls (FC = 3.16).

PIP3 is significantly higher in patients with CTDs than controls

Plasma PIP3 levels were measured through competitive inhibition enzyme immunoassays with a PIP3 ELISA Kit in 95 patients with CTDs and 85 controls. The median PIP3 was significantly lower in controls than patients with CTDs (p = 0.004), as shown in Table 2. According to rs2517582 genotypes, no significant PIP3 difference was found between patients with CTDs and controls with the GG genotype. In contrast, a significant PIP3 difference was found between patients with CTDs and controls with GA or AA genotypes, as shown in Table 3. The differential PIP3 amount was not calculated for the AA genotype separately in patients with CTDs and controls, because of the low numbers of individuals carrying AA genotype in both groups. However the G allele frequency was significantly higher in controls than patients with CTDs (p = 0.01). Receiver operating characteristic curve analysis indicated a significant AUC = 0.608, with p = 0.029 and cut-off point = 314.28 ng/ml of plasma PIP3.

On the basis of the elevated level of Vars2 expression and the PIP3 quantity in patients with CTDs, prioritization of potential druggable protein in the Vars2-Pic3ca-Akt pathway was required. Through data mining from the UniProt knowledge and KEGG databases, and Vars2, Pic3ca and Akt protein screening, Akt was chosen as a possible potential druggable protein.

Characterization of the active binding site of AKT protein with its activator (PIP3): Arg23, Arg25 and Arg86 are essential stabilizing fingers beside Lys14 residue

PIP3 target proteins contain PH domains, which mediate binding to newly formed PIP3. The best known PIP3 target protein is the serine−threonine kinase Akt. On the basis of the high-resolution X-ray diffraction image (1.4 Å) of bounded BH domain Akt (PDB ID 1H10), we identified the active binding site and its binding PIP3 coordinates. PIP3 binds the PH domain of Akt through salt bridges with Arg23, Arg86 and Lys14, Van der Waals interactions with Arg23, Arg25, Arg86 and Lys14, and multiple conventional H bonds with Arg23, Arg25, Arg86, Lys14, Glu17, Tyr18, Ile19 and Asn53. Means and standard deviations of the dG and Kd of the bound PIP3 were computed with KDEEP, as shown in interactive 2D in Figure 2.

Identification of 322PESB as a new PIP3 antagonist: receptor-based pharmacophore feature model

Herein, pharmacophore features were used to annotate the structural physiochemical features necessary for

Table 2: Difference in PIP3 amounts (ng/ml) between patients with CTDs and controls.

Group	PIP3 (ng/ml)	Minimum	Maximum	Kolmogorov−Smirnov Z	P value
Patients with CTDs (n = 95)	293.03 ± 42.5	194.1	356.8	1.75	0.004[a]
Controls (n = 85)	234.30 ± 50.6	133.3	306.3		

[a] This Asymp. Sig. (two-tailed) with Mann−Whitney test.

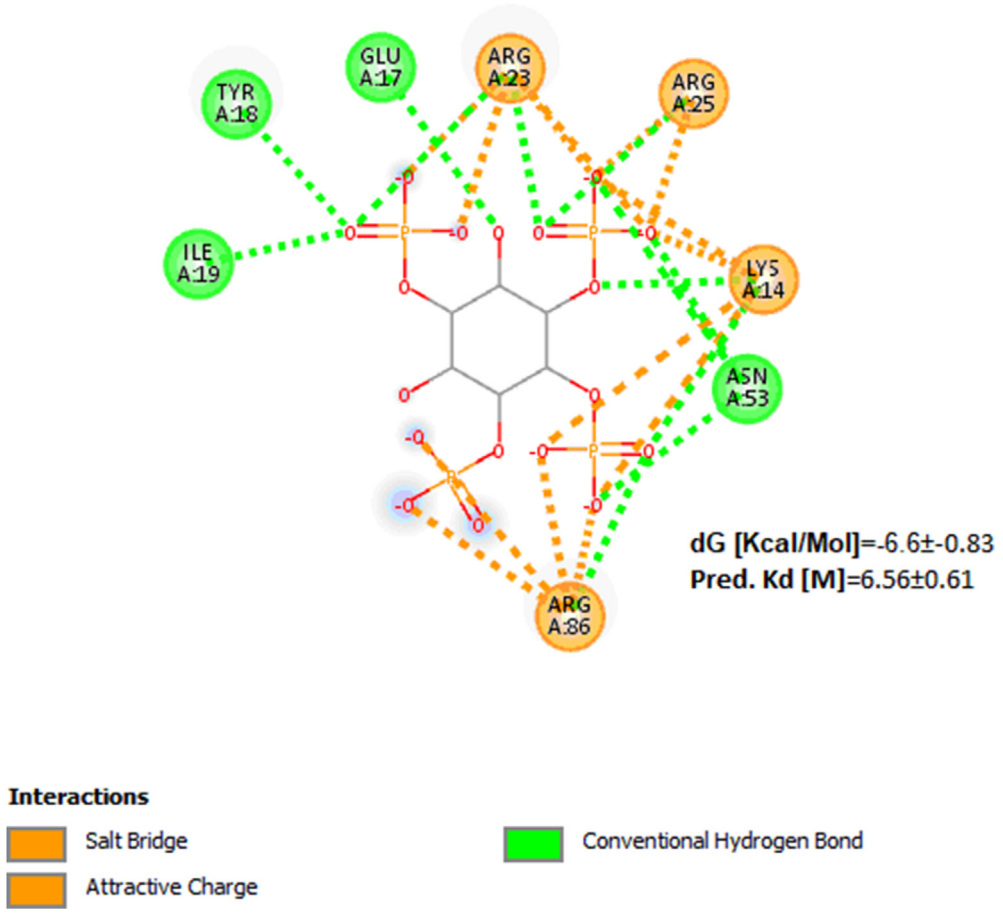

Figure 2: Bonding capacity of the binding site of AKT protein PIP3.

molecular recognition of PIP3 as an inducer by the PH domain of Akt as a receptor. On the basis of five pharmacophore features, a model of the PIP3 binding site was constructed, and an in-house database of 21 small molecules was generated, considering hydrogen bond acceptors, hydrogen bond donors, hydrophobicity, ionizability, charge and solvent accessible area.

Subsequently, the 21 small molecules were assessed according to the SwissADME drug-likeness parameters and Lipinski's rule of five at pH = 7.2. According to SwissADME and Lipinski's rule analysis, 4 of 21 small molecules were considered to be drug-like.

Further sorting based on virtual screening matrices led to prioritize only one drug-like molecule, which was named according to IUPAC with BIOVIA draw as 3-[2-(2-phosphonocyclohexyl) ethylsulfanyl] benzoic acid (322PESB). The docking prioritization was performed on the basis of dG, Kd and Ki. ADME and Lipinski's rule assessment for 322PESB is shown in Figure 3.

322PESB analogues: ADME fit value approach as further sorting to 322PESB drug-likeness

Using an archetype topological molecular fingerprint considering all fragments of the molecular structure, we applied the SwissSimilarity server and data mining of known drugs in the DrugBank database that directly target Akt, to determine known similar drugs and bioactive molecules to 322PESB. We extracted three known small molecules, one bioactive molecule and two drugs similar to 322PESB: (i) 4-(2-hydroxyphenylsulfinyl)-butylphosphonic acid (DB07925), with a chemical structure similarity score of 0.48, which is known to target the tryptophan synthase alpha chain of *Salmonella* typhimurium; (ii) Enzastaurin, with Akt targeting similarity; and (iii) Resveratrol, with weaker chemical structure similarity than DB07925. The ADME values of the three similar small molecules supported that 322PESB was potentially drug-like. The fit values are provided in Table 4.

Superimposition of the novel docked 322PESB binding site against known docked PIP3 binding sites

It well known that the bound ligand substantially affected the binding site conformation. Therefore, superimposition difference between the known docked PIP3 and novel docked 322PESB reflectes the intensive impact of bounded ligand on Akt binding site conformation. On the basis of PDB ID 1H10, we compared docked PIP3 and 322PESB to validate the ability of 322PESB to compete with PIP3. RMSD, solvent accessibility, binding site radius and binding coordinates were considered in the comparison of induced

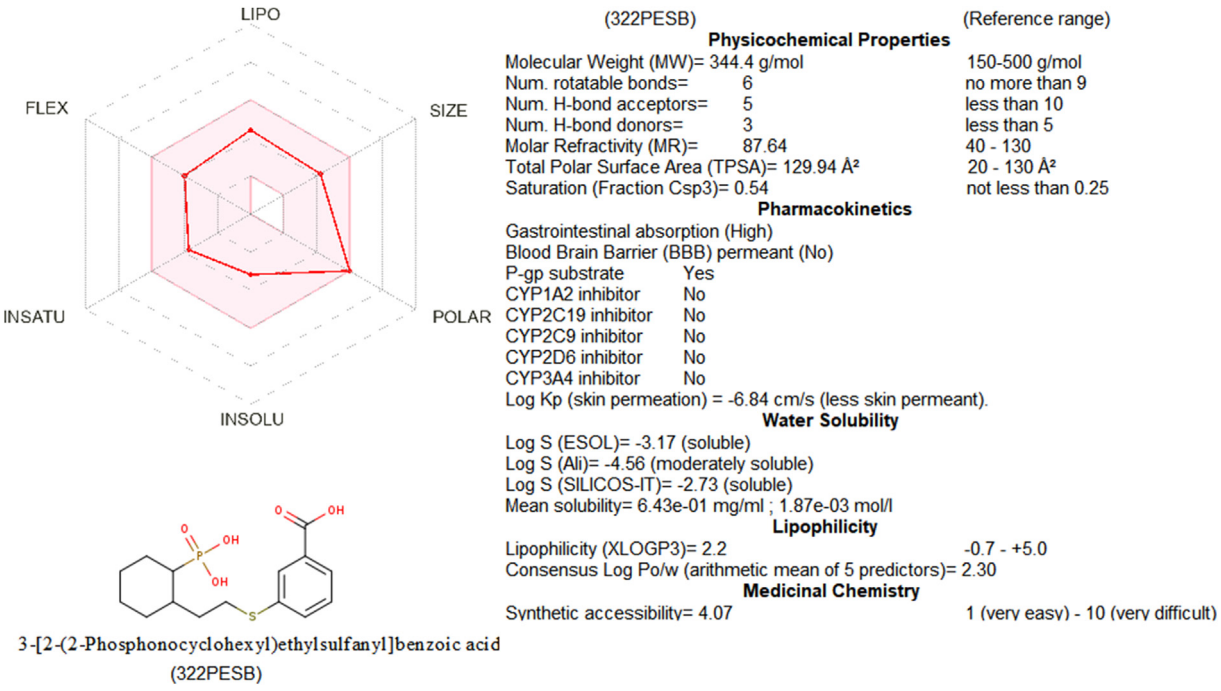

Figure 3: ADME and Lipinski's rules assessment for 322PESB.

Table 4: Overview of fitted ADME values between 322PESB and similar drugs.

ADME values	322PESB analogues			322PESB
	DB07925	Enzastaurin	Resveratrol	
MW	278.26	515.60[a]	228.24	344.4
Fraction Csp3	0.30	0.22	0	0.54
Rotatable bonds	3	5	2	6
H-bond acceptors	5	4	3	5
H-bond donors	3	1	3	3
TPSA	94.83	72.16	60.69	129.94
XLOGP3	3	3.68	3.13	2.2
Consensus log P	2.89	3.58	2.48	2.30
Silicos-IT solubility (mg/ml)	3.42E-08	3.42E-07	1.18E-01	6.43E-01
Silicos-IT solubility (mol/l)	5.18E-07	6.64E-10	5.16E-04	1.87E-03
GI absorption	High	High	High	High
Pgp substrate	No	Yes	No	Yes
CYP450 inhibitor	No	3 Yes 2 No	3 Yes 2 No	No
Lipinski violation	0	1	0	0
Synthetic accessibility	4.01	3.94	2.02	4.07

[a] Values are outside the known corresponding reference range. As shown, all ADME values of 322PESB were within the range of the referenced analogues values; therefore, it was considered a potentially bioactive drug like compound.

conformation change. Almost no induced conformation change occurred during ligand transition from PIP3 as reference to a new 322PESB, as shown in Table 5 and Figure 4.

No significant known off-targets identified for 322PESB

To avoid any adverse effects of 322PESB, we performed screening of this molecule with the SwissTargetPrediction server. Off-target analysis indicated low off-target effects of 322PESB. The closest off-target proteins showed predicted proteins with a probability = 0.111501865. Therefore, 322PESB appears to be a safe and unique ligand for Akt protein.

Discussion

According to Fayez (2018), overstimulation of the Pic3ca-AKT signalling pathway due to altered CTCF-binding affinity and upregulation of the VARS2 gene are associated with CTD pathogenesis.[5] Herein, we tested Fayez's hypothesis experimentally through measurement of the

Table 5: Superposition matrix comparison between docked PIP3 and 322PESB.

Parameter	322PESB			PIP3
Total solvent accessibility (TSA by probe radius = 1.40)	1,807.44			1,571.21
RMSD of interacting residues in Å	C-Alpha (CA)	Main chain (MC)	Side chain (SC)	Reference
Lys14	0.151	0.158	0.151	
Gly16	0.182	0.179	——	
Glu17	0.180	0.183	0.166	
Tyr18	0.202	0.203	0.203	
Ile19	0.212	0.206	0.222	
Arg23	0.179	0.173	0.194	
Arg25	0.152	0.148	0.169	
Asn53	0.154	0.151	0.155	
Arg86	3.886	3.998	7.066	
RMSD for all residues	2.640	2.494	3.766	
Coordinates of ligand binding site	14.86			15.25
X	25.54			24.67
Y	16.87			15.96
Z				
Radius	6.27			6.29

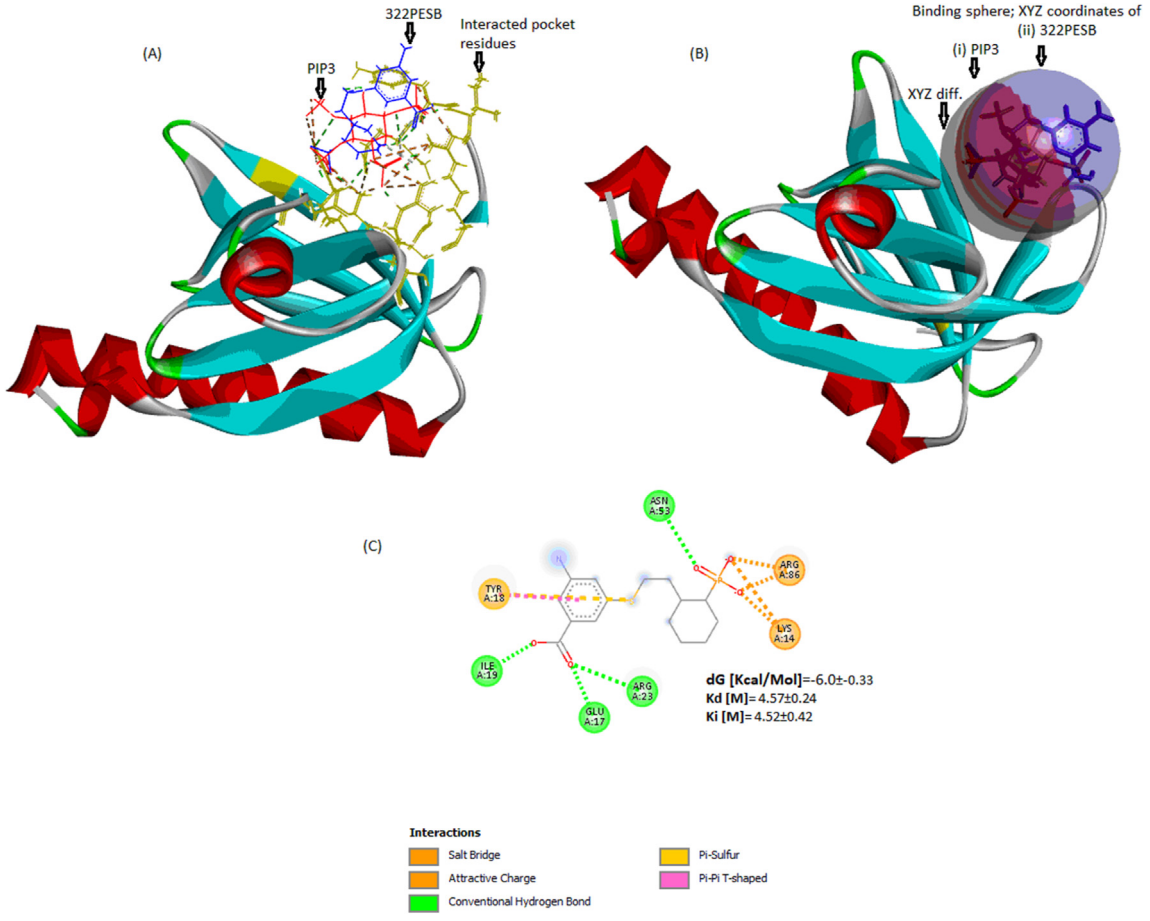

Figure 4: Superimposition of binding sites of docked 322PESB and PIP3. In (A), PIP3 in red and 322PESB in blue are superposed, and interacting Akt residues indicated with arrows. (B) Differential XYZ coordinates of the PIP3 and 322PESB binding sphere, showing little considered difference between PIP3 and 322PESB coordinates. Therefore, 322PESB is considered a potential antagonist for PIP3 and has a dissociation constant (Kd = 4.57) less than that of PIP3 (Kd = 6.56), with a relative dKd = 1.99 M, as shown in (C).

relative Vars2 expression level and PIP3 quantification. The FC of Vars2 was found to be threefold higher in patients with CTDs than controls, and significant PIP3 elevation was observed in plasma samples of patients with CTDs. The A allele of rs2517582 was associated with significantly higher PIP3 in patients with CTDs than controls. Therefore, PIP3

may serve as a potential prognostic factor for CTDs in children. Several studies have indicated that PIP3 is a prognostic factor for patients with cancer.[21–23] The above results were consistent with Fayez's hypothesis, thus supporting the rational discovery of drugs targeting the PIP3 binding site on Akt kinase protein.

Akt is a serine/threonine protein kinase comprising an N-terminal lipid-binding PH domain with specificity for PIP3 and phosphatidylinositol-3,4-bisphosphate.[24] Phosphorylation of Akt by phosphoinositide-dependent kinase 1 (PDK1) begins after recruitment of Akt by PIP3 in the plasma membrane.[25] According to the differential PIP3 concentration between patients with CTDs and controls experimentally determined herein, PIP3 was significantly elevated in patients with CTDs. Therefore, decreasing cellular levels of PIP3 with small molecules targeting Akt is expected to inhibit Akt plasma membrane recruitment; hence, developing a therapeutic small molecule for patients with CTDs with elevated PIP3 should be feasible.

We designed an orally active small molecule PIP3 antagonist, called 322PESB, which was screened through 21 in-house lead small molecules according to the pharmacophore features of the PIP3 binding site on the PH domain of Akt protein. The 322PESB compound has a binding affinity lower by 0.6 kcal/mol than that of PIP3, as predicted by AutoDock Vina. However, 322PESB has a predicted mean Kd 1.99 M less than that of than PIP3; hence, 322PESB shifts the equilibrium state toward Akt-322PESB complex formation at a higher rate than Akt-PIP3 complex formation. Notably, the predicted mean Ki of 322PESB was 4.52 M.

Miao et al. (2010) have discovered a new structural class of nonphosphoinositide small molecules that antagonize PIP3, thereby suppressing the PI3K-PDK1-Akt pathway and triggering metabolic stress and apoptosis; This molecule has been experimentally validated to inhibit tumour growth and induction of apoptosis.[10] Previous studies have been aimed at decreasing elevated PIP3 levels in glioblastoma tumour tissues,[26] and triciribine phosphate has been tested to block recruitment of Akt in the plasma membrane.[27] In the current work, we adopted 322PESB because of its ability to shift the equilibrium of interaction of PH domain /Akt to toward non-phosphorylated Akt complex in patients with CTDs with elevated PIP3.

Herein, we used a receptor-based pharmacophore feature model because of its ability to identify structurally diverse hit compounds binding conformations with relatively low RMSD changes, and because it has previously been used in discover cardiovascular drugs.[11]

Targeting of proteins with small molecules is difficult because active binding sites in proteins are usually flat with multiple interacting pocket residues; therefore, targeting hot spot residues in the binding site and identification of involved non-covalent bonds provide an alternative approach to obtaining active inhibitors.[28] We identified the bonding ability of PIP3 to bound with the PH domain of Akt protein. Arg23, Arg25, Arg86 and Lys14 were identified as essential residues in the PIP3-PH domain Akt stabilization. Therefore, optimization of 322PESB considered those key stabilizing residues. The 322PESB compound forms salt bridges, Van der Waals interactions and conventional hydrogen bonds with Arg23 and Arg86, plus Pi-sulfure and hydrophobic stacking with Tyr18 were bonded decreasing Kdof 322PESB molecule. Thus, 322PESB is predicted to be an efficient PIP3 antagonist drug.

Here, 322PESB was found to reside in the conventionally favourable Lipinski drug-like chemical space and SwissADME drug-likeness features. 322PESB showed characteristics of oral bioactive molecules, including high GI absorption, high cell membrane penetration otherwise-blood−brain barrier, lack of inhibition of cytochrome P450 (CYP) enzymes, inability to serve as a substrate for permeability p-glycoprotein and an acceptable synthetic accessibility score. Notably, 322PESB does not change the PIP3 binding site conformation except for Arg86, according to differential superimposed RMSD scores.

Conclusion

The current results support Fayez's hypothesis regarding a new Vars2-Pic3ca-AKT pathway associated with CTD pathogenesis. PIP3 is therefore a potential prognostic factor for paediatric patients with CTDs. The 322PESB compound may be considered as a drug to decrease phosphorylated Akt kinase protein in patients with CTDs with elevated plasma PIP3. The receptor-based pharmacophore feature model used in the current work may also be appropriate for designing drugs for other enzymes. A allele of the rs2517582 variant is most associated with patients with CTDs. We recommend continuing 322PESB development in future studies.

Source of funding

The National Research Centre (NRC), EGYPT, under project no. 12060177supported this work.

Conflict of interest

No author has any potential or actual conflicts of interest regarding the present article.

Ethical approval

The study protocol was ethically approved by the medical research ethics committee under approval no. 19257 (date: December 2019).

Authors' contributions

AF conceptualized and designed the study; wrote the initial and final revised draft of the article; and designed the drug-like small molecule. NNE analysed and interpreted gene expression data. EAA examined and registered participants' clinical data. MMR analysed and interpreted participants' genotype data. RSL extracted participants' RNA content and measured RNA matrices. HAR quantized and interpreted PIP3 content. MOR supervised and confirmed participants' clinical traits and reviewed the final manuscript. All authors have critically reviewed and approved the final

draft and are responsible for the content and similarity index of the manuscript.

Acknowledgment

The authors acknowledge all participants and their parents.

References

1. Tang B. Single nucleotide polymorphism (SNP) and its preview. **J of Cell Signal 2016**; 1: 22–26. https://doi.org/10.4172/2576-1471.1000129.
2. Kannry J, Williams M. Integration of genomics into the electronic health record: mapping terra incognita. **Genet Med 2013**; 15: 757–760. https://doi.org/10.1038/gim.2013.102.
3. Sanseau P, Agarwal P, Barnes M, Pastinen T, Richards J, et al. Use of genome-wide association studies for drug repositioning. **Nat Biotechnol 2012**; 30: 317–320. https://doi.org/10.1038/nbt.2151.
4. Knight J, Spain S, Capon F, Hayday A, Nestle F, et al. Conditional analysis identifies three novel major histocompatibility complex loci associated with psoriasis. **Hum Mol Genet 2012**; 21: 5185–5192. https://doi.org/10.1093/hmg/dds344.
5. Fayez A. Using postgenome-wide association study analysis; Vars2-Pic3ca-AKT is novel putative interactive pathway associated with conotruncal heart defects. **Biomed Biotechnol Res J 2018**; 2: 269–275. https://doi.org/10.4103/bbrj.bbrj_106_18.
6. Wang J, Yuan Y, Zhou Y, Guo L, Zhang L, et al. Protein interaction data set highlighted with human Ras-MAPK/PI3K signaling pathways. **J Proteome Res 2008**; 7: 3879–3889. https://doi.org/10.1021/pr8001645.
7. Mendoza M, Er E, Blenis J. The Ras-ERK and PI3K-mTOR pathways: cross-talk and compensation. **Trends Biochem Sci 2011**; 36: 320–328. https://doi.org/10.1016/j.tibs.2011.03.006.
8. Varnai P. Selective cellular effects of overexpressed pleckstrin-homology domains that recognize PtdIns (3,4,5)P3 suggest their interaction with protein binding partners. **J Cell Sci 2005**; 118: 4879–4888. https://doi.org/10.1242/jcs.02606.
9. Berndt N, Yang H, Trinczek B, Betzi S, Zhang Z, et al. The Akt activation inhibitor TCN-P inhibits Akt phosphorylation by binding to the PH domain of Akt and blocking its recruitment to the plasma membrane. **Cell Death Differ 2010**; 17: 1795–1804. https://doi.org/10.1038/cdd.2010.63.
10. Miao B, Skidan I, Yang J, Lugovskoy A, Reibarkh M, et al. Small molecule inhibition of phosphatidylinositol-3,4,5-triphosphate (PIP3) binding to pleckstrin homology domains. **Proc Natl Acad Sci USA 2010**; 107: 20126–20131. https://doi.org/10.1073/pnas.1004522107.
11. Arooj M, Sakkiah S, Kim S. A combination of receptor-based pharmacophore modeling & QM techniques for identification of human chymase inhibitors. **PLoS One 2013**; 8:e63030. https://doi.org/10.1371/journal.pone.0063030.
12. National Library of Medicine-Primer Blast - a tool for finding specific primers. http://www.ncbi.nlm.nih.gov/tools/primer-blast. [Accessed 21 October 2019].
13. Daina A, Michielin O, Zoete V. SwissADME: a free web tool to evaluate pharmacokinetics, drug-likeness and medicinal chemistry friendliness of small molecules. **Sci Rep 2017**; 7: 215–217. https://doi.org/10.1038/srep42717.
14. Lipinski C, Lombardo F, Dominy B, Feeney P. Experimental and computational approaches to estimate solubility and permeability in drug discovery and development settings. **Adv Drug Deliv Rev 2012**; 64: 4–17. https://doi.org/10.1016/j.addr.2012.09.019.
15. Murail S, de Vries S, Rey J, Moroy G, Tufféry P. SeamDock: an interactive and collaborative online docking Resource to assist small compound molecular docking. **Front Mol Biosci 2021**; 8: 11–15. https://doi.org/10.3389/fmolb.2021.716466.
16. PlayMoleculeTM One-click molecular discovery. https://www.playmolecule.com/. [Accessed 21 April 2022].
17. BIOVIA, Dassault Systèmes, BIOVIA Workbook, Release. *BIOVIA pipeline pilot*. San Diego: Dassault Systèmes; 2020. . [Accessed 25 April 2022].
18. SwissParam. https://www.expasy.org/resources/swissparam. [Accessed 1 July 2022].
19. Bragina ME, Daina A, Perez MAS, Michielin O, Zoete V. The SwissSimilarity 2021 web tool: novel chemical libraries and additional methods for an enhanced ligand-based virtual screening experience. **Int J Mol Sci 2022**; 23: 811–813. https://doi.org/10.3390/ijms23020811.
20. Gfeller D, Grosdidier A, Wirth M, Daina A, Michielin O, et al. SwissTargetPrediction: a web server for target prediction of bioactive small molecules. **Nucleic Acids Res 2014**; 42: W32–W38. https://doi.org/10.1093/nar/gku293.
21. Zhong Y, Zhang J, Zhou Y, Mao F, Lin Y, Xu Y, Guan J, Shen S, Pan B, Wang C, Peng L, Huang X, Li Y, Cao X, Sun Q. Phosphatidylinositol-3,4,5-Trisphosphate dependent rac exchange factor 1 (PREX1) is a novel predictor of prognosis for breast cancer patients: a Retrospective case series. **Med Sci Mon Int Med J Exp Clin Res 2019**; 25: 6554–6562. https://doi.org/10.12659/MSM.915845.
22. Marquard FE, Jücker M. PI3K/AKT/mTOR signaling as a molecular target in head and neck cancer. **Biochem Pharmacol 2020**; 172:113729. https://doi.org/10.1016/j.bcp.2019.113729.
23. Molinari F, Frattini M. Functions and Regulation of the PTEN gene in colorectal cancer. **Front Oncol 2014**; 3: 326. https://doi.org/10.3389/fonc.2013.00326.
24. Thomas C, Deak M, Alessi D, van Aalten D. High-resolution structure of the pleckstrin homology domain of protein kinase B/Akt bound to phosphatidylinositol (3,4,5)-trisphosphate. **Curr Biol 2002**; 12: 1256–1262. https://doi.org/10.1016/s0960-9822(02)00972-7.
25. Stokoe D. Dual Role of phosphatidylinositol-3,4,5-trisphosphate in the activation of protein kinase B. **Science 1997**; 277: 567–570. https://doi.org/10.1126/science.277.5325.567.
26. Cheng C, Fan Q, Weiss W. PI3K signaling in Glioma-animal models and therapeutic challenges. **Brain Pathol 2009**; 19: 112–120. https://doi.org/10.1111/j.1750-3639.2008.00233.x.
27. Garrett C, Coppola D, Wenham R, Cubitt C, Neuger A, et al. Phase I pharmacokinetic and pharmacodynamic study of triciribine phosphate monohydrate, a small-molecule inhibitor of AKT phosphorylation, in adult subjects with solid tumors containing activated AKT. **Invest N Drugs 2010**; 29: 1381–1389. https://doi.org/10.1007/s10637-010-9479-2.
28. Wong S, Baron R, McCammon J. Hot-spot residues at the E9/Im9 interface help binding via different mechanisms. **Biopolymers 2008**; 89: 916–920. https://doi.org/10.1002/bip.21035.

How to cite this article: Fayez AG, Esmaiel NN, Ashaat EA, Refeat MM, Lotfy RS, Raouf HA, El Ruby MO. New drug-like small molecule antagonizes phosphatidylinositol
(3,4,5)-trisphosphate (PIP3) in patients with conotruncal heart defects. J Taibah Univ Med Sc 2023;18(6):1244–1253.